MIND THE GAP - DIFFERENCE BETWEEN CENSORED AND UNCENSORED ELECTRIC VEHICLE CHARGING DEMAND

A PREPRINT

Frederik Boe Hüttel, Filipe Rodrigues and Francisco Câmara Pereira

December 21, 2022

ABSTRACT

Electric vehicle charging demand models, with charging records as input, will inherently be biased toward the supply of available chargers, as the data do not include demand lost from occupied stations and competitors. This lost demand implies that the records only observe a fraction of the total demand, i.e. the observations are censored, and actual demand is likely higher than what the data reflect. Machine learning models often neglect to account for this censored demand when forecasting the charging demand, which limits models' applications for future expansions and supply management. We address this gap by modelling the charging demand with probabilistic censorship-aware graph neural networks, which learn the latent demand distribution in both the spatial and temporal dimensions. We use GPS trajectories from cars in Copenhagen, Denmark, to study how censoring occurs and much demand is lost due to occupied charging and competing services. We find that censorship varies throughout the city and over time, encouraging spatial and temporal modelling. We find that in some regions of Copenhagen, censorship occurs 61% of the time. Our results show censorship-aware models provide better prediction and uncertainty estimation in actual future demand than censorship-unaware models. Our results suggest that future models based on charging records should account for the censoring to expand the application areas of machine learning models in this supply management and infrastructure expansion.

***K*eywords** Electric mobility, Electric Vehicle charging demand, Latent mobility demand, Bayesian modeling.

1 Introduction

Electric vehicle (EV) charging stations are increasingly more prominent in energy and transportation infrastructure planning [Bauer et al., 2021, Jakobsen et al., 2020], and adequate infrastructure is one of the main barriers to large-scale EV adoption [Yi and Shirk, 2018]. However, planning and expanding charging infrastructure is a complex procedure that needs to account for factors such as charging station placement, demand predictions, and integration with existing power systems and road infrastructure [Deb, 2021]. Recently, machine learning has been used to tackle some of the challenges mentioned above, particularly charging demand predictions, which is a problem well suited for machine learning [Buzna et al., 2019]. Forecasts of the charging demand with machine learning models can inform energy providers and operations of the current stations of the energy requirements.

A distinct property of charging stations is that they are a *shared* service. The shared nature of charging stations has implications for how models forecast the charging demand, as shared mobility services often experience *censorship*, where demand is lost because of limited supply [Hüttel et al., 2022]. Forecasters tend to neglect this concept when modelling the charging demand with historical data, as the observations will depend highly on the available supply and might not reflect the *actual* behaviour of the service users, which introduces biases into the models [Gammelli et al., 2020] and limits their application in strategic expansion.

Specifically, for a charging station with two plugs, the station can never record a demand above two cars charging, even though more cars potentially need to recharge. The capacity of a charging station acts as an upper limit for the demand each station can observe, making the data only contain a fraction of the true unobserved (latent) demand distribution.

Figure 1: The figure shows two examples of how censoring of EV charging demand occurs. Left: Censored demand lost to lost opportunities. Right: Charging demand lost to competing services.

Censorship unawares models do not forecast the unobserved demand; therefore, they can only asses the demand for the current station and not future stations.

Another example of censorship in EV charging demand is that charging station operations lose demand to competing services. Users might decide to use a competing service, which censors the data the service providers observe. Therefore operators might have demand observations which do not reflect the actual demand around their stations, as they lost it to competitors. The censorship-unaware model will limit the operator's ability to make strategic moves in the competitive environment.

For the case of EV charging, we argue that censoring mainly occurs in the two ways mentioned above; firstly, when an EV wants to charge however other cars occupy nearby charging stations[1] [Larsen, 2016], or if a service provider loses demand to a competing service [Li et al., 2021]. Figure 1 illustrate the two scenarios. Basing decisions on censorship-unware models will be biased and produce underestimations of the actual demand, leading to inefficient charging station operation [Gammelli et al., 2022a]. Therefore, we argue that planners of future charging infrastructure must be aware of the gap between the observed- and unobserved demand distributions and account for it in future modelling approaches.

To address this gap, we propose to model the charging demand with censorship-aware models, giving an unbiased estimate of charging demand. Specifically, we focus our modelling on probabilistic censored neural networks due to their flexibility and scalability. We focus our approach on spatial and temporal model architectures, as the demand will likely fluctuate in these two dimensions [Hüttel et al., 2021]. Traditional time series models neglect to account for spatial fluctuations [Kim and Kim, 2021]. We investigate the two censorship scenarios mentioned above, with demand lost to occupied chargers and competing services.

We organise the rest of the work as follows. Section 2 reviews related work on modelling EV charging demand and censored modelling in the transport and machine learning domain. After the review, section 3 introduces two censorship-aware models with different distributional assumptions of the charging demand. Firstly, the classical Tobit model, which assumes a Gaussian demand distribution and secondly, a quantile regression approach which offers a semi-non-parametric distribution fit of the demand. It also covers how to model the spatial and temporal correlations between stations with graph neural networks. The section 4 introduces the data we base our models on, and section 5 describes our experimental setup, where we compare censorship-aware models with unaware models. In section 6, we discuss some of the advantages and limitations of our modelling approach. Lastly, section 7 concludes our main findings and outlines future research directions.

2 Related Work

Modelling EV charging demand is a complex problem and has been studied from many angles, such as simulation-based modelling [Jin et al., 2023], queuing theory [Rich et al., 2022] and applications of statistical models [Amara-Ouali et al., 2022]. In this review, we focus on applications of machine learning models to model the charging demand. Lastly, we cover censored modelling approaches in the machine learning context and the mobility demand setting.

2.1 Electric Vehicle Charging Demand.

Previous studies of EV charging demand, varies spatially from the scale of a single station [Zhu et al., 2019] to city-wide [Li et al., 2021], and all the way to country-level demand predictions [Kim and Kim, 2021]. Temporally

[1] Often referred to as frustrated demand.

the forecasting horizon also varies between a short-term forecast of 15 minutes to day-ahead forecasting and even longer-term for expansion planning, often dictated by the application of the model.

A substantial point of variability is the machine learning and statistical models themselves. Traditional statistical models, such as Autoregressive Integrated Moving Average (ARIMA and variations thereof), have been used to forecast the EV charging demand [Amini et al., 2016, Louie, 2017], with extensions to non-parametric estimation based on quantile regression [Buzna et al., 2021, Huber et al., 2020]. Statistical models often provide interpretable parameters of the input features, which is helpful for policy and decision-making. However, machine learning models tend to show better predictive performance at the cost of interpretability [Buzna et al., 2019]. Many machine learning models have often been used to model the demand, with random forest [Almaghrebi et al., 2020, Lu et al., 2018, Ullah et al., 2021], support vector machines [Almaghrebi et al., 2020, Majidpour et al., 2016, Sun et al., 2016, Xydas et al., 2013], and gradient boosting [Almaghrebi et al., 2020, Buzna et al., 2019] as the primary models. The modelling often includes temporal and external features to improve predictive performance. Over the last few years, recurrent neural networks (RNN), a recurrent variation of neural networks that learn a signal's temporal features, have been used in demand forecasting due to their ability to handle large datasets [Yi et al., 2021]. Specifically, the long short-term memory (LSTM) variation is extensively used to forecast demand [Boulakhbar et al., 2022, Kim and Kim, 2021, Ma and Faye, 2022, Van Kriekinge et al., 2021, Zhu et al., 2019]. However, they are restricted by their temporal aspect, as they do not capture the complex spatial correlations between individual charging stations. Therefore, researchers are applying temporal graph neural networks, which combine LSTMs and graph convolutions, to use spatial and temporal features in the forecast [Hüttel et al., 2021, Li et al., 2021].

A last point of variety is the datasets used for modelling the demand. In general, there is a lack of open-world charging datasets due to privacy or data property issues regarding charging records, leading researchers to other data sources to estimate charging demand. Tu et al. [2016] used GPS trajectories to estimate the EV charging demand from electric taxis in Shenzhen, China, by modelling the energy consumption of taxis and the dynamics of charging stations. Another example is Li et al. [2021], which uses the daily traffic flow to estimate the proportional charging demand of cars. Recently, researchers have started to use *observed* charging records from charging stations as a basis for the demand [Amara-Ouali et al., 2022, Boulakhbar et al., 2022, Buzna et al., 2021, Flammini et al., 2019, Hüttel et al., 2021, Kim and Kim, 2021, Ma and Faye, 2022, Van Kriekinge et al., 2021]. The charging records are an efficient way to estimate the energy and power demand of the charging stations to inform energy providers [Boulakhbar et al., 2022]. However, these models will not extrapolate outside the supply, limiting their application to infrastructure expansion.

When the charging records are the basis for demand modelling, the data will inherently be biased by the availability and supply of chargers [Gammelli et al., 2020, Hüttel et al., 2022]. Moreover, the data does not account for demand lost to competing services. Consequently, the *actual* charging demand is typically latent (i.e., unobserved), and its observations are likely to lie below it. Namely, they are *right-censored*. This censoring will be important when the charging station operators need to plan expansion, provide waiting time predictions, or schedule maintenance operations [Gammelli et al., 2022b].

2.2 Censored Modeling of Mobility demand

Gaussian processes (GP) have previously been the go-to model for modelling censored distributions in the mobility research field [Gammelli et al., 2020, 2022a]. The GP offers a probabilistic fit of the latent demand distribution, assuming it follows a Gaussian distribution with a Tobit likelihood function. However, the GP faces some scalability modelling limitations when the dataset size becomes too large [Liu et al., 2020]. As an alternative to the GP, censored variations of SVM [Shim and Hwang, 2009] and random forest [Li and Bradic, 2020] exist, which are yet to be applied in mobility research.

The trend in transportation research and EV charging demand modelling is that researchers increasingly use larger datasets, which forces models to be able to scale [Mao et al., 2016, van Cranenburgh et al., 2022]. Therefore, in earlier work [Hüttel et al., 2022], we propose to model the latent demand distribution using neural networks with a censored quantile regression approach, leveraging their flexible nonlinear modelling capabilities. The censored quantile neural network assumes an asymmetric Laplace likelihood function which is common in Bayesian inference of censored quantile regression Yang et al. [2016], Yu and Stander [2007]. It does not assume any parametric form of the latent demand distribution, and the demand can follow a non-symmetrical distribution. An advantage of using neural networks is also that they scale to large datasets and can fit multiple data modalities [Goodfellow et al., 2016, LeCun et al., 2015]. Outside the mobility demand context, censored quantile neural networks have been applied to biomedical data [Jia and Jeong, 2022, Pearce et al., 2022]. As highlighted by Hüttel et al. [2022] and Pearce et al. [2022], the applications of censored neural networks are scarce.

In conclusion, we have not found any studies on modelling the censored EV charging demand in a machine learning context, despite the prevalence of censorship in transportation research, demand settings and shared mobility services. We propose to estimate the true latent demand distribution of EV charging demand, using the flexibility of neural networks to capture spatial and temporal correlations with temporal graph neural networks.

3 Methodology

Firstly, this section introduces two modelling approaches to model the true latent demand distributions in the context of neural networks: the Tobit model and the censored quantile regression model. We present the likelihood functions for both of these under right censorship. Afterwards, we cover how to capture the spatial-temporal correlations structures with temporal graph neural networks and combine the models with the likelihood functions.

3.1 Censored modelling

A dataset consisting of n observations with features $\{\mathbf{x}_i, \ldots, \mathbf{x}_n\}$ and a corresponding set of target variables $\{y_i, \ldots, y_n\}$, is censored if the target values are clipped observations of a corresponding latent (true) value $\{y_i^*, \ldots, y_n^*\}$. For each observation, there exist a threshold value $\{\tau_1, \ldots, \tau_N\}$, which makes observations either left-censored or right-censored, such that:

$$y_i = \begin{cases} y^*\,, & y_i^* > \tau_i \\ \tau_i\,, & y_i^* \leq \tau_i \end{cases} \text{ in left-censorship,} \tag{1}$$

$$y_i = \begin{cases} y^*\,, & y_i^* < \tau_i \\ \tau_i\,, & y_i^* \geq \tau_i \end{cases} \text{ in right-censorship.} \tag{2}$$

The threshold value τ_i can be either observed, unobserved, fixed or stochastic [Hüttel et al., 2022]. In right censoring, τ_i will act as an upper limit for the observations, and in left censoring, a lower limit. In the case of EV charging demand, the observations will often be right censored based on the current supply.

3.2 Parametric Distribution estimation.

A commonly used model for censored modelling is the *Tobit* model [Tobin, 1958]. The model assumes that the latent value, y^*, follows a Gaussian distribution. In the context of neural networks, a Tobit model estimates both a mean function $\mu_\beta(\mathbf{x_i})$ and a standard-deviation function $\sigma_\beta(\mathbf{x}_i)$:

$$f_\beta(\mathbf{x}_i) = \mathcal{N}(y_i^* | \mu_\beta(\mathbf{x}_i), \sigma_\beta(\mathbf{x}_i))\,. \tag{3}$$

Where $\sigma_\beta(\mathbf{x}_i)$ is constraint to positive values. The parameters β can be estimated with back-propagation on the negative log-likelihood of the censored distribution. The likelihood for a right-censored Tobit model is given by:

$$\mathcal{L}\left(y|\beta, \mathbf{x}\right) = \prod_{i=1}^{n} \left\{ \frac{1}{\sigma(\mathbf{x}_i)} \varphi\left(\frac{y_i - \mu(\mathbf{x}_i)}{\sigma(\mathbf{x}_i)} \right) \right\}^{(1-l_i)} \left\{ 1 - \Phi\left(\frac{y_i - \mu(\mathbf{x}_i)}{\sigma(\mathbf{x}_i)} \right) \right\}^{l_i}, \tag{4}$$

where φ is the Probability Density Function (PDF) of a $\mathcal{N}(0,1)$, Φ is its Cumulative Distribution Function (CDF), and for a given fixed threshold τ_i:

$$l_i = \begin{cases} 0\,, & y_i < \tau_i \\ 1\,, & y_i = \tau_i \end{cases}. \tag{5}$$

Which leads to the corresponding negative log-likelihood function

$$\log \mathcal{L}\left(y|\beta, \mathbf{x}\right) = -\sum_{i=1}^{n} l_i \log\left(\frac{1}{\sigma(\mathbf{x}_i)} \phi\left(\frac{y_i - \mu(\mathbf{x}_i)}{\sigma(\mathbf{x}_i)} \right) \right) + (1 - l_i) \log\left(1 - \Phi\left(\frac{y_i - \mu(\mathbf{x}_i)}{\sigma(\mathbf{x}_i)} \right) \right). \tag{6}$$

3.3 Non-Parametric Distributions

A non-parametric distribution can be modelled through censored quantile regression [Yu and Stander, 2007] as an alternative to the parametric Gaussian assumption. Quantile regression estimates the θ-quantile of the true latent distribution, and multiple quantiles can be combined to model the distribution entirely. Naturally, the θ must be constrained to $0 < \theta < 1$. Then $q_{\theta,i}$ will be the θ-quantile estimate of the label y_i^*:

$$f_\beta(\mathbf{x}_i) = q_{\theta,i}\,. \tag{7}$$

For a quantile regression model with left censorship and a specified quantile θ, the following likelihood function can be used for Bayesian Inference of the parameters β [Yu and Stander, 2007]:

$$\mathcal{C}\left(y|\beta,\mathbf{x},\theta\right) = \theta^N\left(1-\theta\right)^N \exp\left\{-\sum_{i=1}^{N}\rho_\theta\left(y_i - \max\left\{\tau_i, \hat{q}_{i,\theta}\right\}\right)\right\}, \tag{8}$$

Where ρ_θ is the tilted loss:

$$\rho_\theta(r) = \max\{\theta r\,, (\theta-1)r\}\,. \tag{9}$$

A problem with quantile regression (Equation 7) is that one model only fits a single quantile, and multiple models must be estimated to learn the entire target distribution. However, a whole set of quantiles $\{q_{k,\theta}\}_{k=1}^K$ can be jointly estimated using multi-output neural networks without adding substantial computational cost. We get the following likelihood model with multi-output for the censored quantile regression for the extension. [Hüttel et al., 2022]

$$\mathcal{C}\left(y|\beta,\mathbf{x},\{\theta_k\}_{k=1}^K\right) = \sum_{k=1}^{K}\left(\theta_k^N\left(1-\theta_k\right)^N \exp\left\{-\sum_{i=1}^{N}\rho_{\theta,k}\left(y_i - \max\left\{\tau_i, \hat{q}_{\theta,k,i}\right\}\right)\right\}\right). \tag{10}$$

Since the likelihood functions above are based on left censoring, we negate the target values to make the right censoring scheme into a left censoring one.

3.4 Spatial-Temporal Modeling

Spatial modelling We propose to model the demand with temporal graph neural networks to model the spatial and temporal correlation structures between charging stations [Zhao et al., 2020]. As the name implies, the spatial structure is modeled using a *graph*, $G = (N, E)$, where $V = \{v_1, v_2, \ldots, v_m\}$ is a set of nodes and E is the set of edges between the nodes.

For a graph with m nodes and a temporal signal $\mathbf{x}_t \in \mathbb{R}^{m\times c}$ at timestep t, where c is the set of additional input, the spatial-temporal modelling can be formulated as using the last L timesteps, to forecast the next Q timesteps. [Tygesen et al., 2022]

$$f_\beta(G; \mathbf{x}_{t-L+1:t}) = p(\mathbf{x}_{t+1:t+Q}|G; \mathbf{x}_{t-L+1:t}, \beta)\,. \tag{11}$$

We model G as a weighted graph, using the geographical locations of nodes and the distance between them. We model the weights of an edge between the two nodes i and j as:

$$e_{ij} = \exp(-h(z_i, z_j)) \tag{12}$$

Where z_i and z_j are the latitude and longitude of the nodes and h is the *Haversine Distance* between the nodes in km [Hüttel et al., 2021]. The set E defines the adjacency matrix $A \in R^{m\times m}$, representing the network's topology. To capture features from the topological structure, a graph convolutional network (GCN) uses graph convolutions to model the relationship between nodes in a graph [Kipf and Welling, 2016]. A 2-layered GCN model is formulated as follows:

$$f(A, \mathbf{x}_t) = \sigma\left(\widehat{A}\ \mathrm{Relu}\left(\widehat{A}\mathbf{x}W_0\right)W_1\right)\,, \tag{13}$$

where X is the feature matrix, A is the adjacency matrix, $\widehat{A} = \widetilde{D}^{-\frac{1}{2}}\widetilde{A}\widetilde{D}^{-\frac{1}{2}}$ denotes a preprocessing step, $\widehat{A} = A + I_N$ is a matrix with self-connection structure, and $\widetilde{D}$ is a degree matrix, $\widetilde{D} = \sum_j \widetilde{A}_{ij}$. W_0 and W_1 are the weight matrices in the first and second layers, respectively, and $\sigma(\cdot)$, $\mathrm{Relu}()$ is the activation function [Zhao et al., 2020].

Temporal Modeling The GCN extends to a temporal signal by combining the GCN with long short-term memory layers (T-GCN) [Hochreiter and Schmidhuber, 1997, Zhao et al., 2020]. The key equations of the T-GCN with an LSTM cell can be summarised as follows, where $f(A, \mathbf{x}_t)$ is the graph convolution from Equation 13:

$$i_t = \sigma_g\left(W_i f(A, \mathbf{x}_t) + U_i h_{t-1} + b_i\right) , \tag{14}$$
$$f_t = \sigma_g\left(W_f f(A, \mathbf{x}_t) + U_f h_{t-1} + b_f\right) , \tag{15}$$
$$o_t = \sigma_g\left(W_o f(A, \mathbf{x}_t) + U_o h_{t-1} + b_o\right) , \tag{16}$$
$$\tilde{c}_t = \sigma_c\left(W_c f(A, \mathbf{x}_t) + U_c h_{t-1} + b_c\right) , \tag{17}$$
$$c_t = f_t \odot c_{t-1} + i_t \odot \tilde{c}_t \, , \tag{18}$$
$$h_t = o_t \odot \sigma_h\left(c_t\right) . \tag{19}$$

The matrices W_{i-c} and U_{i-c} and the vectors b_{i-c} contain the trainable weights, $\odot$ denotes the Hadamard product and $c_0 = 0$ and $h_0 = 0$. f_t is the forget gate activation, i_t is the input/update gate activation and o_t is the output gate hidden activation. σ_g is the sigmoid function and σ_c and σ_h are the hyperbolic tangent activation function [Hochreiter and Schmidhuber, 1997].

In summary, the T-GCN models capture the complex topological structure using the GCN and the temporal structure of the data using the LSTM layers [Zhao et al., 2020]. The output from the T-GCN is a set of values for each node in the graph. We combine the T-GCN with the censored likelihood functions from Equation 6 and Equation 10, to compute the loss for each node and sum them.

4 Counterfactual study

Let us now introduce a *counterfactual* study based on GPS-trajectories of internal combustion engine cars (ICE) in the metropolitan area of Copenhagen, Denmark. These trajectories will be the basis for estimating both observed and unobserved charging demand in the city. We assume that the ICE cars are electric and generate a fleet of EVs, where we model how the state-of-charge (SoC) of the vehicles will vary based on the GPS trajectories. We include charging dynamics from the public charging station, where cars can recharge, similar to the approach proposed by [Tu et al., 2016]. This study provides us with the *true* unobserved charging demand, and we can assess the censorship levels that occur throughout space and time. We call it a counterfactual study because we essentially ask the question "what would have happened with charging demand if the ICE Cars from the dataset had been EVs instead". We summarise the counterfactual study in Algorithm 1 and cover each step in depth in Appendix A.

4.1 Data

As mentioned, the data consist of GPS trajectories from ICE cars in Denmark, where locations are saved every 20 seconds. Each GPS location contains an ID of the car and can be stitched together into a complete GPS trajectory, which forms a trip for the car. Each trip contains a start coordinate, an end coordinate, and the distance driven by a car. Cars' parking time can be inferred as the time between trips. To ensure the users' privacy, the trajectories are randomised by adding a noise distance between 50 and 500 meters to each trip's endpoints. The GPS trajectories of the cars were collected over three months, from September to November 2019 and is uniformly distributed across the country (Denmark) and vehicle segments. The GPS trajectories do not suffer from the biases identified in other EV studies, namely, having early adopters bias the behaviour in the data sets. In total, 32664 cars are observed in the capital region (Copenhagen), which accounts for 5.71% of the cars in the city (A total of 571627 cars for the period [Statistik-Banken, 2022]). In the observations period, the penetration rate of EVs in Copenhagen was 1%, and for the fall of 2022, the penetration rate has increased to 2.5% [Statistik-Banken, 2022]. We visualise the number of daily trips for the entire period in Figure 2. In total, we have 1.5 million trips with a median of 10 trips pr. car.

Charging Stations in Copenhagen To model the charging infrastructure in Copenhagen, we use the charging infrastructure from 2021. We scraped the infrastructure from uppladdning [2021], an open-source map containing locations of EV charging stations. The scraped chargers have different charging power ranging from slow chargers with 3.7 kW charging to fast chargers with 150 kW. These provide us with the locations and the power for each charging station in the city, which we use to determine where the ICE cars would have charged, assuming they were EVs.

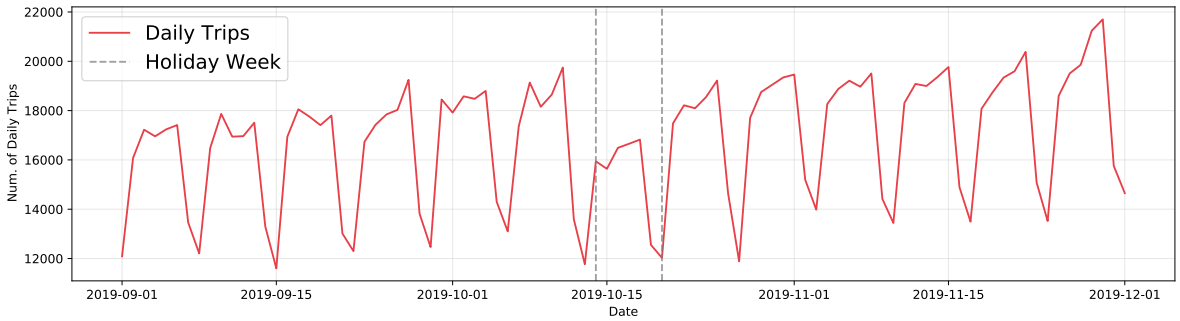

Figure 2: Overview of the total number of daily trips in the dataset. From the 14'th to the 20th of October, there is a drop in daily trips due to it being a holiday week in Denmark. Therefore, there are fewer trips due to a reduced traffic flow from commuting.

4.2 Queuing Models

As already explained, we theorise that the observed demand is censored by lost opportunities when charging stations are occupied. We, therefore, implement three different queues to handle multiple cars wanting to charge as follows:

- *Gas-station*: People queue up like an ordinary gas station and wait for their turn to charge. The EVs charge to 80% SoC before driving away. This behaviour is primarily associated with fast chargers and is often referred to as a smart queue [Monta, 2021].
- *3-Hour*: In this queue, people are only allowed to charge for 3 hours before driving away, regardless of the SoC of the car. Cars that arrive at an occupied station will not be charged. This behaviour reflects policies (e.g. Denmark [FDM, 2022]) where there is a (typically 3 hrs) time limit for parking and charging.
- *First comes - First serve queue*: The last queue is a first come, first serve queue, where the EV who comes first charges for the entire duration until the next trip. Cars that arrive at an occupied station will not be charged. This corresponds to opportunistic behaviour.

These variations of queues will naturally give rise to different levels of censoring. For example, the gas-station queue will be able to serve all users, given that they have time to wait. We also keep the queue similar across all charging stations.

4.3 Outline of the counterfactual study

We sample different numbers of cars from the GPS trajectories to match different EV penetration rates. The GPS trajectories have a penetration rate of 5% for all cars. In 2019, The penetration rate of EVs was roughly 1% and in 2022, is roughly 3%. Therefore, we vary the penetration rate between 1% to 5% and test the three different queuing models. Using the sampled cars and the queuing model, we model how the cars would have charged given they were EVs. We sample the battery sizes according to the the market distribution of different EV types (section A.1). We compute their willingness to charge based on the SoC consumption of a trip. The charging stations is selected probabilistic from the five closest charging stations, at an end trip. Each car follows the procedure outlined in Algorithm 1.

4.4 Demand Profiles from counterfactual study

We now turn to the output of the counterfactual study, focusing on the censored part of the charging demand. For each GPS trajectory, we stored the energy demand observed and unobserved, which we will use to model the censored demand. We report the fraction of hours where censorship occurs in Table 1, across the queue and the penetration rate.

Across all the different queues and penetration rates, we observe that demand is censored at different scales. The gas-station queue offers a very low level of censorship due to the nature of charging, where observations are only censored if the EVs have a new trip while in the queue. When we go to the different queues, we see that amount of censoring increases. For current penetration levels of EVs, we find that between 33% and 53% of hours censoring occurs in the entire area. As the penetration rate increases, censorship follows, which is a natural consequence, as the infrastructure would need to expand to handle more demand from chargers.

Algorithm 1 Overview of the counterfactual study.

Generate a fleet of electric vehicles.
Set queuing model.
Set SoC for the fleet of cars $SoC \sim \mathcal{N}(0.6, 0.2), 0.20 \leq SoC \leq 1$.
for each GPS trajectory **do**
    Find the car id of the GPS trajectory.
    Compute energy consumption for the car.
    Update SoC-level for the car.
    Compute willingness to charge for the car.
    Compute were to charge based on the end location of the trip.
    Add car to queue.
    Compute energy demand based on the time spent charging.
    Save the energy demand from the charging event.
end for

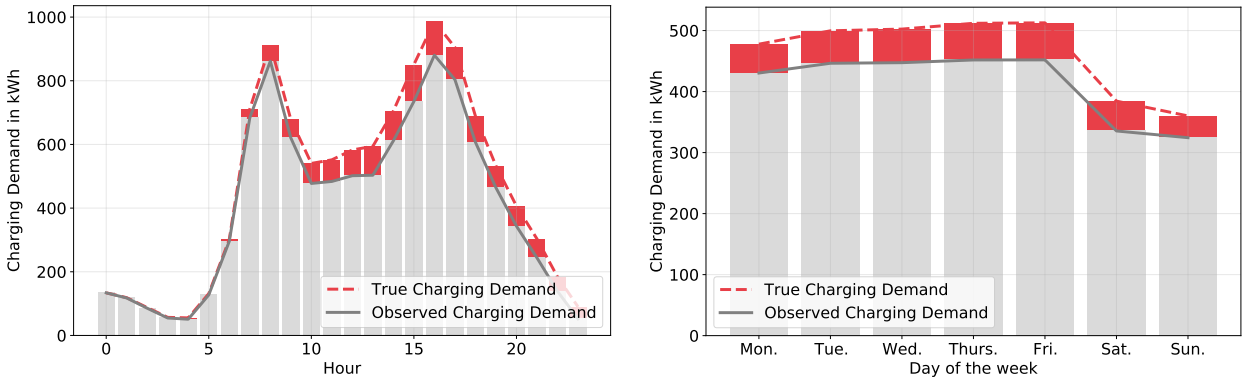

Figure 3: Average charging demand, either grouped by the time of day (left) or day of the week (right). Rate: 5% and queue: *First come - First serve*.

Based on the study, we find that in the temporal dimension, most censoring occurs during peak demand hours, both in the morning and afternoon (Figure 3). The peak demand hours reflect the traffic patterns of the original GPS trajectories and are similar to what other studies observe in charging demand in cities [Hüttel et al., 2021]. The demand also varies throughout the week, with lower demand on weekends than on ordinary weekdays. Even though the demand varies throughout the week, the amount of censored demand is generally stable. There is no large discrepancy in the proportional censored demand over the different weekdays (Figure 3).

As a final step, we aggregate the demand spatially. We conduct *kmeans* clustering of all the charging stations to divide the city into ten regions. Each cluster centre will work as the temporal graph neural network nodes. We do this for modelling purposes, as demand at an individual charging station can be very random and sporadic.Figure 4 shows the spatial overview of the counterfactual study.

Based on the counterfactual study, censorship also varies in spatial dimensions. In Table 2, we show the censorship levels for the 5%-penetration of EVs and the *First come - first serve* queue. In cluster 0 (The western part of Copenhagen), 61% of the hourly charging demand is censored. These large censorship levels stem from only two regional charging stations covering a large spatial area. Still, it does not have sufficient capacity to meet the demand in this

Queue	Penetration rate				
	1% (Historical)	2%	3% (Current)	4%	5% (Data)
Gas-station Queue	<0.1%	2.2%	4.9%	9.8%	16.4%
3 Hour queue	4.1%	17.6%	33.2%	46.8%	56.9%
First come - First serve Queue	8.3%	30.1%	53.2%	66.2%	70.5%

Table 1: Fraction of hours where the observed demand is censored for the different queuing models.

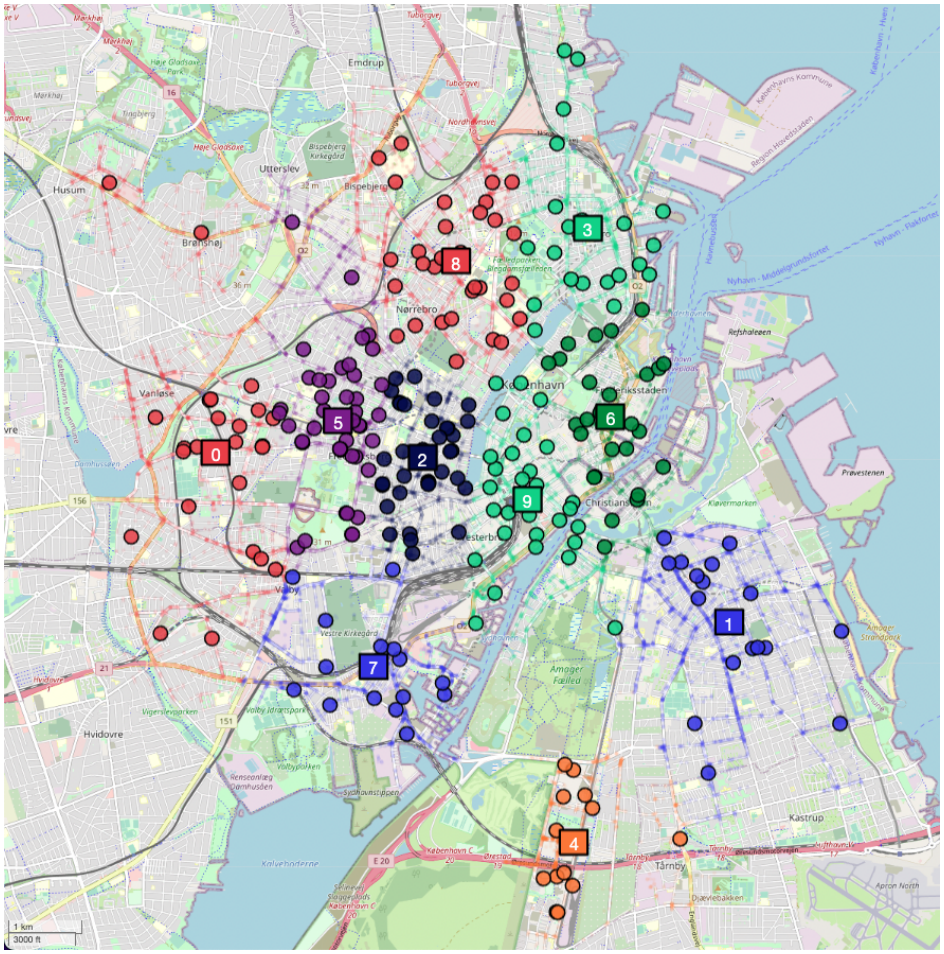

Figure 4: Overview of the spatial structure in the counterfactual study. Small circles indicate the end of the GPS trajectories. The circle with a dark line is the charging station, and squares indicate the centroids of the clusters. Colours indicate which cluster they belong to.

area. This area is residential, so most of the demand could be served by home charging, which s not included in our study. In contrast, in cluster 4 (The southern part of Copenhagen), we find lower censorship levels and rarely any demand at night. Cluster 4 is an industrial area with low demand at night (Figure 5). We report the censorship across all the different queues, penetration rates and clusters in Appendix B.

In summary, based on GPS trajectories from ICE cars in the fall of 2019, we have created a *counterfactual* study of the charging behaviour in this period. The study allows us to assess the true *latent* charging demand, which is un-observed if only the charging records are used. The study did employ some simplifications of the battery and the choice modelling assumptions to generate the demand profiles.

5 Experiments and Results

This section introduces our experimental setup. First, we experiment with the censoring schemes from Table 1 and model the demand for the entire city. We compare the censorship-aware models to the unaware ones before we test the models in a competitive environment where only a fraction of the demand is observed.

We denote the models based on their likelihood functions used to model. We include two censorship-unaware models; a *Gaussian* model fitted with maximum likelihood and a *quantile* regression (QR) model with the uncensored tilted loss (Equation 9). We compare them to censorship-aware models; *Tobit* (Equation 6) and a *censored QR* (Equation 10). We keep the same architectural design choices across all the models and use the same random seed for their initialisation of parameters. Each experiment is conducted ten times, and the reported results are the average across these runs.

Cluster	Location	% of censored hours
0	Western part of city	61.03%
1	South Easter part	20.29%
2	West of the city centre	3.12%
3	North Eastern part of the city	16.31%
4	Southern part of the city	11.28%
5	Western part of city	24.33%
6	North part of the city centre	6.57%
7	South Western part of the city	20.16%
8	North Western part of the city	31.17%
9	City center	16.67%

Table 2: Table showing the fraction of hours with censored observation with 5% EV penetration and First-come Queue.

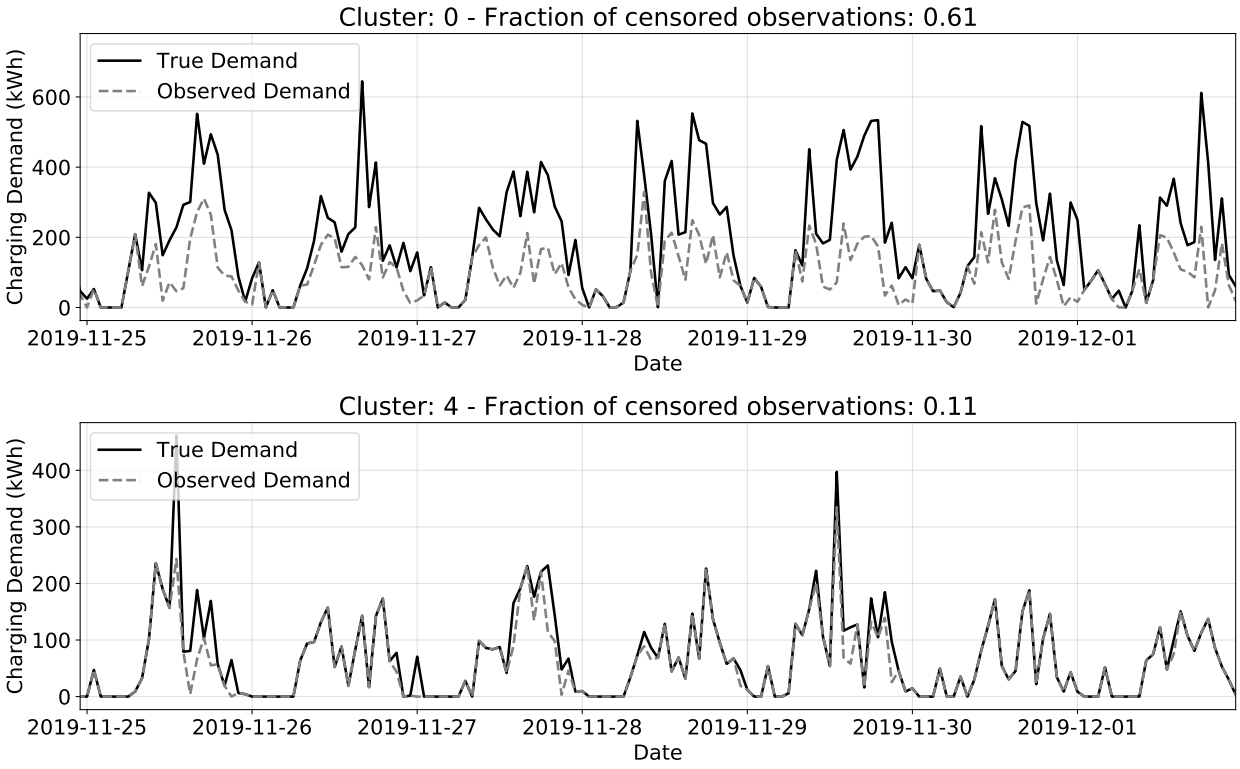

Figure 5: Charging demand from the Counterfactual study for cluster 0 and cluster 4 in the city.

5.1 Architectures

For the input size of the temporal signal, we use the last 168 hourly demand observations, which equals one week of data. In addition, we add the type of day and hour as external input features, encoded into cyclical features using sine and cosine. We combine the cyclical features with the historical demand to create time series for each node in the graph G. We scale each time series between 0 and 1 to avoid nodes contributing a large weight to the loss function during training [Zhao et al., 2020]. We use 16 and 8 channels for the graph convolutions and an LSTM with 32 hidden units. We use the Adam optimiser [Kingma and Ba, 2014] with a learning rate of 0.0003 and norm clipping of 1.0. We train each model for 1000 epochs with a 256 batch size and apply an early stopping criterion of 0.001 on the validation loss.

We divide the dataset into a train, validation and test set with a split of 80%, 10% and 10%, respectively. For the quantile regression models, we estimate 0.05, 0.5, and 0.95-quantiles. All the models are implemented in Keras, [Chollet et al., 2015] and the graph convolutions are implemented using StellarGraph [Data61, 2018].

Queue	Penetration rate	1.0%	2.0%	3.0%	4.0%	5.0%
Gas-station	Gaussian	0.798	0.800	0.710	0.782	0.714
	Tobit	0.801	0.802	0.712	0.774	0.713
	QR	0.657	**0.719**	**0.668**	0.731	**0.680**
	Censored QR	**0.655**	0.720	0.670	**0.731**	0.681
3-hour	Gaussian	0.766	0.752	0.812	0.781	0.798
	Tobit	0.764	0.750	0.800	0.763	0.765
	QR	0.644	0.678	0.756	0.740	0.763
	Censored QR	**0.641**	**0.673**	**0.748**	**0.726**	**0.736**
First come - First serve	Gaussian	0.696	0.776	0.797	0.887	0.945
	Tobit	0.694	0.773	0.751	0.784	0.790
	QR	0.577	0.697	0.734	0.841	0.894
	Censored QR	**0.574**	**0.690**	**0.709**	**0.774**	**0.765**

Table 3: Tilted loss summed for all the nodes. Lower is better, and the best-performing model is highlighted in bold.

5.2 Evaluation Metrics

We evaluate our models on the tilted loss they achieve on the test set. We compute their quantiles for the Gaussian and Tobit models using the estimated distributions. In addition, we evaluate our models based on the following metrics, commonly used for quantile regression evaluation: Interval Coverage Percentage (ICP) and Mean Interval Length (MIL). We limit the notation to a single node in the graph:

$$\text{ICP} = \frac{1}{N}\sum_{j=1}^{N}\begin{cases}1 & \text{if } \hat{q}_{i,\theta} \leq y_i \leq \hat{q}_{i,\theta'} \\ 0 & \text{otherwise}\end{cases} \tag{20}$$

$$\text{MIL} = \frac{1}{N}\sum_{j=0}^{N}(|\hat{q}_{i,\theta} - \hat{q}_{i,\theta'}|) \tag{21}$$

The desired quality of a probabilistic model is to have a high ICP (Equation 20), which is close to 0.9, meaning that 90% of observations are within the prediction interval while keeping a low MIL (Equation 21), making the model predictions precise.

5.3 Total demand predictions

Firstly, we experiment with evaluation on all charging stations and nodes with the censoring scheme reported in Table 1. For the experiments, we vary the penetration rate of EVs, and as mentioned above, the censorship levels increase as the penetration rate increases and the queuing model changes. We report the tilted loss on the true demand for the test set in Table 3.

The quantile regression-based models (QR and Censored-QR) generally yield a lower tilted loss for the test set. There is no clear distinction between the censorship-aware and unaware models for the Gas-station queue due to the generally low levels of censorship we observe for this type of queue. However, as we vary the queue and the censorship levels, we find that the discrepancy between the censorship-aware and unaware models increases. In general, the Censored QR is the best-performing model for the 3-hour and First come queue, where the censorship levels increases.

In Figure 6, we depict the MIL and ICP for the models across the different queues and penetration rates. Since the amount of censoring varies between nodes, the ICP will be pictured for the cluster with the most censoring. The Gaussian models (Gaussian and Tobit) tend to have higher ICP and MIL, meaning they tend to have larger prediction intervals. As a consequence, a higher ICP compared to the non-parametric models. The QR models tend to have a tighter confidence interval (lower MIL), with an ICP comparable to the Gaussian models. Notice that the best model is one with ICP close to 90% and the shortest MIL possible.

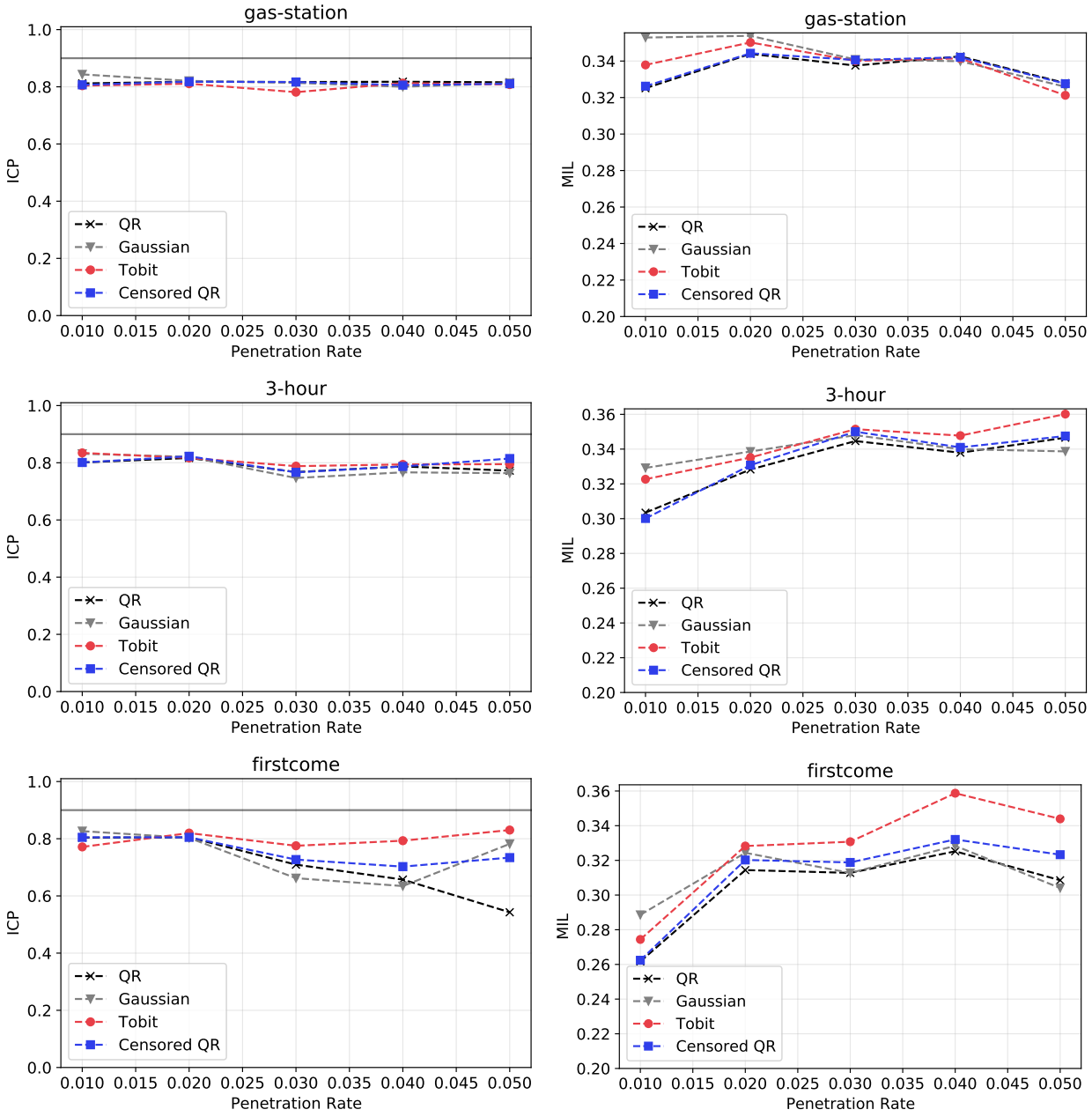

Figure 6: The ICP (left) and MIL (right) across the different penetration rates and Queues. In general, the ICP should be close to 0.9 with a lower MIL value, which means that the uncertainty can capture the target distribution while allowing for uncertainty in the predictions.

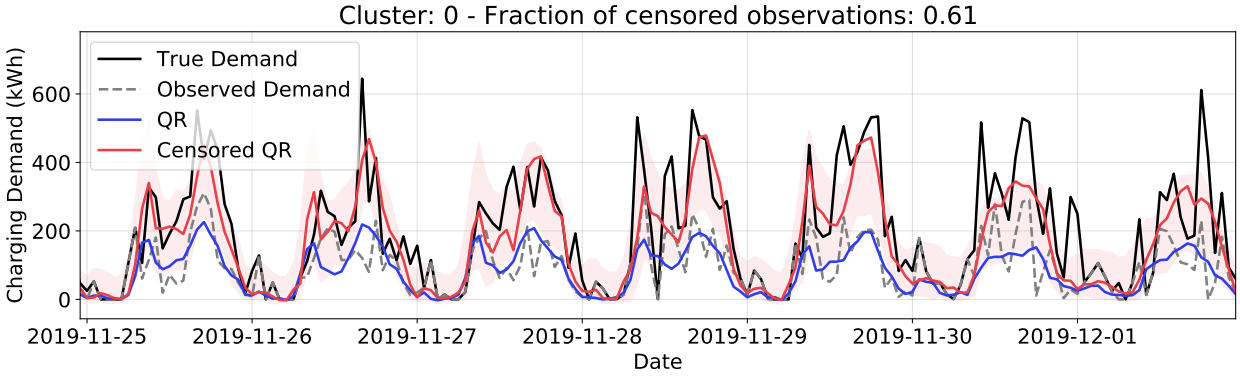

Figure 7: Demand predictions for cluster 0 for the first-come queue with 5% penetration rate.

5.4 Application of censored demand modelling

Here we describe some of the benefits of using the censorship-aware model compared to the censorship-unaware and give an example of its influence on future expansion plans. Infrastructure expansion planning is more complex than we present here, but we highlight the benefits of using censorship-aware models.

Again, we turn to cluster 0, where a large fraction of observations is censored. We find that, in general, the censored QR has a better fit of the actual true demand than the censorship-unaware QR (Figure 7). The QR model provides a relatively accurate fit of the observed demand and tens to forecast the demand sufficiently by forecasting the general temporal patterns. However, the censored QR provides higher predictions of the charging demand than the system observes. These elevated predictions indicate that potentially expanding the infrastructure in cluster 0 is viable.

A particular benefit of the censorship-aware models is their estimate of the capacity increase needed to serve the true demand. The gap between the predicted demand and observed censored could already serve as an indicator for expansion. Still, the regressed value and their corresponding uncertainty provide a size of the additions required to meet all demand. In conclusion, the censorship-aware models estimate the capacity required to meet demand, which provides a reasonable basis for data-driven decisions. Flexible supply could also serve peak demand hours due to the variation of demand throughout the day.

5.5 Competing Services

We now focus on a scenario with multiple EV charging providers in a competitive environment. We focus our experiment and models from the perspective of one single charging service provider, i.e., we only observe a fraction (market share) of the total charging demand in the city and then try to forecast the true demand for operation expansions.

We experiment with different amounts of market shares, ranging from 10% up to 95%, with 10% market share meaning that 90% of the true demand is unobserved. We also do not assume the number of competitors in the market but only use data observed by one provider. We cluster the chargers into graph nodes as described. For all the chargers, we sample the market share of chargers in the entire city and censor all the charging stations.

We report the tilted loss, ICP, and MIL in Table 4 for the different levels of market share. We find that the censorship-aware models outperform their unaware counterparts. For low market shares, we find that the Tobit model tends to provide a better fit of the demand, but as the market-share increase, the censored QR models surpass it across all the evaluation metrics. Again, the uncertainty reflected in the prediction intervals is tighter than the Tobit model while still having a high percentage of observations within its forecasts.

These results show the benefit of using censorship-aware models in a competitive environment. They provide a good basis for the charging stations' operations and estimates of the demand the competitors can serve. Naturally, this estimate of competitors' demand provides a competitive edge for future expansions and operation of the infrastructure from a charging station operator's point of view, as the estimation of the demand lost to competitors can be used for strategic moves [Li et al., 2021].

Metric	Model	Market share 10%	25%	50%	75%	95%
TL	Gaussian	4.428	2.658	1.370	0.920	0.734
	Tobit	**3.085**	**1.898**	1.092	0.842	0.729
	QR	4.217	2.522	1.265	0.851	0.669
	Censored QR	3.248	1.904	**1.060**	**0.790**	**0.671**
ICP	Gaussian	0.325	0.446	0.589	0.689	0.800
	Tobit	**0.314**	**0.496**	0.724	0.786	0.804
	QR	0.259	0.492	0.632	0.717	0.819
	Censored QR	0.355	0.564	**0.679**	**0.760**	**0.809**
MIL	Gaussian	0.223	0.321	0.320	0.312	0.315
	Tobit	**0.319**	**0.427**	0.398	0.352	0.324
	QR	0.179	0.277	0.300	0.302	0.316
	Censored QR	0.302	0.375	**0.347**	**0.331**	**0.320**

Table 4: Model performance as we increase market share. Bold indicates the model with the lowest Tilted loss.

6 Discussion

Throughout the analysis, experiments and results, we have argued that the observed charging demand from charging records is censored and therefore does not reflect the demand for EV charging. We used ICE GPS trajectories and battery models to support the hypothesis to conduct a counterfactual study. This counterfactual study allows us to investigate how much of the charging demand is censored versus what is observed.

The counterfactual study does have the advantage over artificial censoring of the data that the censoring happens as a consequence of the charging infrastructure and not just as censoring of the dataset, which is common practice in censored modelling [Gammelli et al., 2020, Hüttel et al., 2022]. We argue that the censoring from the study is coherent with real-world censoring and provides a more accurate censoring scheme than artificial censoring. Another advantage is the use of ICE GPS trajectories, which are not biased by the behaviour of early EV adopters, as the charging behaviour of the EVs does not constrain the ICE. Therefore, the GPS trajectories represent the desired behaviour from users when they are not constrained to charging their cars. The counterfactual study provides some modelling advantages compared to using public charging records.

However, the counterfactual study does employ simplistic charging and battery models. A future research direction is to evaluate and incorporate the other key travel metrics influencing EVs' energy consumption, such as speed, acceleration and ambient temperature [McNerney et al., 2017]. All of these factors lead to variations in the battery consumption for each trip of the cars; therefore, we underestimate charging demand, as the SoC of the EVs is likely lower than what we present here [Hipolito et al., 2022]. This supports the argument that EV charging demand is censored and that the censoring is larger than the one we observe, emphasising the need for censorship-aware models in modelling EV charging demand.

7 Conclusion and future research directions

In summary, we have argued that the charging demand observed by charging records is censored due to opportunities lost to competition or supply limitations. This lost demand is often neglected in the EV charging demand modelling, and it will impact the application of machine learning models in infrastructure expansion. The gap between lost and observed demand must be addressed to facilitate efficient and cost-effective expansions.

We have presented several methods to account for this censoring in modelling EV charging demand. We propose to model the demand with neural networks which are flexible and scalable. To evaluate both censorship scenarios, we conduct a counterfactual study of Copenhagen, where ICE cars are assumed to be EVs following different penetration rates, to infer the EV charging demand. For the highest penetration with the most ineffective queue, we find that 61% of all hours the demand is censored.

Through experiments on the demand, we showed that the censorship-aware models showed superior modelling performance in the true latent distribution of charging demand than censorship-unaware models. Across the three different queues with found that the censored quantile regression model performed the best by having a lower tilted loss across

the different experiments compared to the Tobit model. Only for the gas-station queue, where censorship is low, did the censorship-unaware models perform. We also compare censorship-aware and unaware models in a competitive environment with different market share amounts, where the censorship-aware models were superior in modelling the demand.

In future work, we plan to improve upon the counterfactual study by including complex choice models with realistic charging behaviours in users, as users might not want to queue up for slow charging opportunities. We also plan to incorporate other key travel metrics, such as speed, acceleration, road grade and temperature, to more accurately estimate the consumption of state of charge. We propose to use empirical charging profiles instead of the piece-wise linear function used in this work. In future works, we plan to evaluate the impact of censored modelling in operation and expansion of the charging stations, focusing on mobile charging stations.

8 Acknowledgements

The research leading to these results has received funding from the Independent Research Fund Denmark (Danmarks Frie Forskningsfond) under grant no. 0217-00065B.

References

Almaghrebi, A., Aljuheshi, F., Rafaie, M., James, K., and Alahmad, M. (2020). Data-driven charging demand prediction at public charging stations using supervised machine learning regression methods. *Energies*, 13(16).

Amara-Ouali, Y., Goude, Y., Hamrouche, B., and Bishara, M. (2022). A benchmark of electric vehicle load and occupancy models for day-ahead forecasting on open charging session data. In *Proceedings of the Thirteenth ACM International Conference on Future Energy Systems*, e-Energy '22, page 193–207, New York, NY, USA. Association for Computing Machinery.

Amini, M. H., Kargarian, A., and Karabasoglu, O. (2016). Arima-based decoupled time series forecasting of electric vehicle charging demand for stochastic power system operation. *Electric Power Systems Research*, 140:378–390.

Bauer, G., Hsu, C.-W., Nicholas, M., and Lutsey, N. (2021). Charging up america: Assessing the growing need for u.s. charging infrastructure through 2030.

Boulakhbar, M., Farag, M., Benabdelaziz, K., Kousksou, T., and Zazi, M. (2022). A deep learning approach for prediction of electrical vehicle charging stations power demand in regulated electricity markets: The case of morocco. *Cleaner Energy Systems*, page 100039.

Buzna, L., De Falco, P., Ferruzzi, G., Khormali, S., Proto, D., Refa, N., Straka, M., and van der Poel, G. (2021). An ensemble methodology for hierarchical probabilistic electric vehicle load forecasting at regular charging stations. *Applied Energy*, 283:116337.

Buzna, L., De Falco, P., Khormali, S., Proto, D., and Straka, M. (2019). Electric vehicle load forecasting: A comparison between time series and machine learning approaches. In *2019 1st International Conference on Energy Transition in the Mediterranean Area (SyNERGY MED)*, pages 1–5.

Chollet, F. et al. (2015). Keras. `https://github.com/fchollet/keras`.

Data61, C. (2018). Stellargraph machine learning library. `https://github.com/stellargraph/stellargraph`.

Database, T. E. (2021). Source: `https://ev-database.org/`.

Deb, S. (2021). Machine learning for solving charging infrastructure planning: A comprehensive review. In *2021 5th International Conference on Smart Grid and Smart Cities (ICSGSC)*, pages 16–22.

FDM (2022). Se reglerne for parkering med elbil og plugin-hybrid (transl: *Watch the rules for parkering of Electric cars and plugin-hybrids*).

Flammini, M. G., Prettico, G., Julea, A., Fulli, G., Mazza, A., and Chicco, G. (2019). Statistical characterisation of the real transaction data gathered from electric vehicle charging stations. *Electric Power Systems Research*, 166:136–150.

Gammelli, D., Peled, I., Rodrigues, F., Pacino, D., Kurtaran, H. A., and Pereira, F. C. (2020). Estimating latent demand of shared mobility through censored gaussian processes. *Transportation Research Part C: Emerging Technologies*, 120:102775.

Gammelli, D., Rolsted, K. P., Pacino, D., and Rodrigues, F. (2022a). Generalized multi-output gaussian process censored regression. *Pattern Recognition*, 129:108751.

Gammelli, D., Wang, Y., Prak, D., Rodrigues, F., Minner, S., and Pereira, F. C. (2022b). Predictive and prescriptive performance of bike-sharing demand forecasts for inventory management. *Transportation Research Part C: Emerging Technologies*, 138:103571.

Gjelaj, M., Hashemi, S., Andersen, P., and Træholt, C. (2020). Optimal infrastructure planning for ev fast charging stations based on prediction of user behaviour. *IET Electrical Systems in Transportation*, 10.

Goodfellow, I., Bengio, Y., and Courville, A. (2016). *Deep Learning*. MIT Press. `http://www.deeplearningbook.org`.

Hipolito, F., Vandet, C., and Rich, J. (2022). Charging, steady-state soc and energy storage distributions for ev fleets. *Applied Energy*, 317:119065.

Hochreiter, S. and Schmidhuber, J. (1997). Long short-term memory. *Neural Comput.*, 9(8):1735–1780.

Huber, J., Dann, D., and Weinhardt, C. (2020). Probabilistic forecasts of time and energy flexibility in battery electric vehicle charging. *Applied Energy*, 262:114525.

Hüttel, F. B., Peled, I., Rodrigues, F., and Pereira, F. C. (2021). Deep spatio-temporal forecasting of electrical vehicle charging demand. *CoRR*, abs/2106.10940.

Hüttel, F. B., Peled, I., Rodrigues, F., and Pereira, F. C. (2022). Modeling censored mobility demand through censored quantile regression neural networks. *IEEE Transactions on Intelligent Transportation Systems*, pages 1–13.

Jakobsen, S., Flader, L., Andersen, P., Thingvad, A., and Bollerslev, J. (2020). *Sådan skaber Danmark grøn infrastruktur til én million elbiler: Analyse og anbefalinger fra DEA og DTU, november 2019*. Technical University of Denmark.

Jia, Y. and Jeong, J.-H. (2022). Deep learning for quantile regression under right censoring: Deepquantreg. *Computational Statistics & Data Analysis*, 165:107323.

Jin, Z., Xu, Y., and Li, Z. (2023). Electric vehicle charging demand forecast based on residents' travel data. In *International Conference on Green Intelligent Transportation System and Safety*, pages 401–411. Springer.

Kim, Y. and Kim, S. (2021). Forecasting charging demand of electric vehicles using time-series models. *Energies*, 14(5).

Kingma, D. P. and Ba, J. (2014). Adam: A method for stochastic optimization. cite arxiv:1412.6980Comment: Published as a conference paper at the 3rd International Conference for Learning Representations, San Diego, 2015.

Kipf, T. N. and Welling, M. (2016). Semi-supervised classification with graph convolutional networks. *CoRR*, abs/1609.02907.

Larsen, E. (2016). *Demand response in a market environment*. PhD thesis, Technical University of Denmark, Department of Electrical Engineering.

LeCun, Y., Bengio, Y., and Hinton, G. (2015). Deep learning. *Nature*, 521(7553):436–444.

Li, A. H. and Bradic, J. (2020). Censored quantile regression forest. In *International Conference on Artificial Intelligence and Statistics*, pages 2109–2119. PMLR.

Li, C., Dong, Z., Chen, G., Zhou, B., Zhang, J., and Yu, X. (2021). Data-driven planning of electric vehicle charging infrastructure: A case study of sydney, australia. *IEEE Transactions on Smart Grid*, 12(4):3289–3304.

Liu, H., Ong, Y., Shen, X., and Cai, J. (2020). When gaussian process meets big data: A review of scalable gps. *IEEE Transactions on Neural Networks and Learning Systems*, 31:4405–4423.

Louie, H. M. (2017). Time-series modeling of aggregated electric vehicle charging station load. *Electric Power Components and Systems*, 45(14):1498–1511.

Lu, Y., Li, Y., Xie, D., Wei, E., Bao, X., Chen, H., and Zhong, X. (2018). The application of improved random forest algorithm on the prediction of electric vehicle charging load. *Energies*, 11(11).

Ma, T.-Y. and Faye, S. (2022). Multistep electric vehicle charging station occupancy prediction using hybrid lstm neural networks. *Energy*, 244:123217.

Majidpour, M., Qiu, C., Chu, P., Pota, H. R., and Gadh, R. (2016). Forecasting the ev charging load based on customer profile or station measurement? *Applied Energy*, 163:134–141.

Mao, M., Yue, Y., and Chang, L. (2016). Multi-time scale forecast for schedulable capacity of electric vehicle fleets using big data analysis. In *2016 IEEE 7th International Symposium on Power Electronics for Distributed Generation Systems (PEDG)*, pages 1–7.

McNerney, J., Needell, Z. A., Chang, M. T., Miotti, M., and Trancik, J. E. (2017). Tripenergy: Estimating personal vehicle energy consumption given limited travel survey data. *Transportation Research Record*, 2628(1):58–66.

Monta (2021). Smart queue: Get notified when a charge point becomes availabl.

Observatory, E. A. F. (2021). Directorate-general for mobility and transport - source: https://www.eafo.eu/vehicles-and-fleet/m1#.

Pearce, T., Jeong, J.-H., Jia, Y., and Zhu, J. (2022). Censored quantile regression neural networks for distribution-free survival analysis. In *Advances in Neural Information Processing Systems, NeurIPS*.

Rich, J., Vandet, C. A., and Pilegaard, N. (2022). Cost–benefit of a state-road charging system: The case of denmark. *Transportation Research Part D: Transport and Environment*, 109:103330.

Shim, J. and Hwang, C. (2009). Support vector censored quantile regression under random censoring. *Computational statistics & data analysis*, 53(4):912–919.

Statistik-Banken (2022). Source: Statistik banken - statistics denmark.

Sun, Q., Liu, J., Rong, X., Zhang, M., Song, X., Bie, Z., and Ni, Z. (2016). Charging load forecasting of electric vehicle charging station based on support vector regression. In *2016 IEEE PES Asia-Pacific Power and Energy Engineering Conference (APPEEC)*, pages 1777–1781.

Tobin, J. (1958). Estimation of Relationships for Limited Dependent Variables. *Econometrica*, 26(1):24–36.

Tu, W., Li, Q., Fang, Z., lung Shaw, S., Zhou, B., and Chang, X. (2016). Optimizing the locations of electric taxi charging stations: A spatial–temporal demand coverage approach. *Transportation Research Part C: Emerging Technologies*, 65:172–189.

Tygesen, M. N., Pereira, F. C., and Rodrigues, F. (2022). Unboxing the graph: Neural relational inference for mobility prediction. *CoRR*, abs/2201.10307.

Ullah, I., Liu, K., Yamamoto, T., Zahid, M., and Jamal, A. (2021). Electric vehicle energy consumption prediction using stacked generalization: an ensemble learning approach. *International Journal of Green Energy*, 18(9):896–909.

uppladdning (2021). Source: https://www.uppladdning.nu/.

van Cranenburgh, S., Wang, S., Vij, A., Pereira, F., and Walker, J. (2022). Choice modelling in the age of machine learning - discussion paper. *Journal of Choice Modelling*, 42:100340.

Van Kriekinge, G., De Cauwer, C., Sapountzoglou, N., Coosemans, T., and Messagie, M. (2021). Day-ahead forecast of electric vehicle charging demand with deep neural networks. *World Electric Vehicle Journal*, 12(4).

Xydas, E. S., Marmaras, C. E., Cipcigan, L. M., Hassan, A. S., and Jenkins, N. (2013). Forecasting electric vehicle charging demand using support vector machines. In *2013 48th International Universities Power Engineering Conference (UPEC)*, pages 1–6.

Yang, Y., Wang, H. J., and He, X. (2016). Posterior inference in bayesian quantile regression with asymmetric laplace likelihood. *International Statistical Review*, 84(3):327–344.

Yi, Z., Liu, X. C., Wei, R., Chen, X., and Dai, J. (2021). Electric vehicle charging demand forecasting using deep learning model. *Journal of Intelligent Transportation Systems*, 0(0):1–14.

Yi, Z. and Shirk, M. (2018). Data-driven optimal charging decision making for connected and automated electric vehicles: A personal usage scenario. *Transportation Research Part C: Emerging Technologies*, 86:37–58.

Yu, K. and Stander, J. (2007). Bayesian analysis of a Tobit quantile regression model. *Journal of Econometrics*, 137(1):260–276.

Zhao, L., Song, Y., Zhang, C., Liu, Y., Wang, P., Lin, T., Deng, M., and Li, H. (2020). T-gcn: A temporal graph convolutional network for traffic prediction. *IEEE Transactions on Intelligent Transportation Systems*, 21(9):3848–3858.

Zhu, J., Yang, Z., Mourshed, M., Guo, Y., Zhou, Y., Chang, Y., Wei, Y., and Feng, S. (2019). Electric vehicle charging load forecasting: A comparative study of deep learning approaches. *Energies*, 12(14).

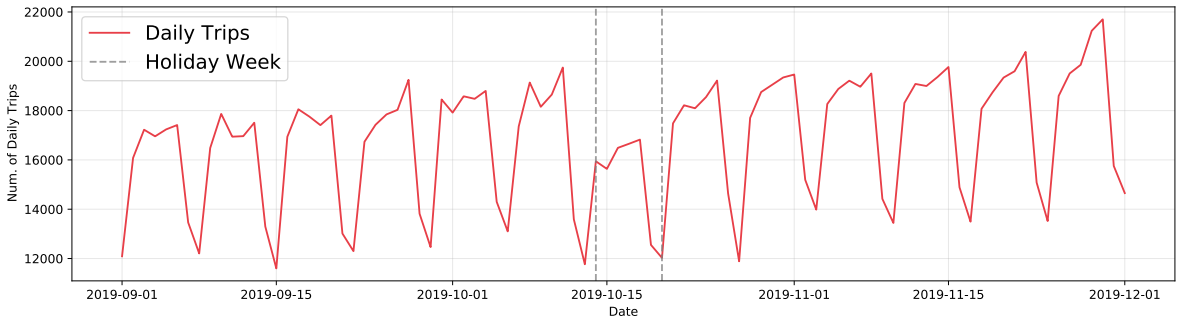

Figure 8: Overview of the total number of daily trips in the dataset. From the 14'th to the 20th of October, there is a drop in daily trips due to it being a holiday week in Denmark. Therefore, there are fewer trips due to a reduced traffic flow from commuting.

A Counterfactual study - appendix

A.1 Data

As mentioned, the data consist of GPS trajectories from ICE cars in Denmark, where locations are saved every 20 seconds. Each GPS location contains an ID of the car and can be stitched together into a complete GPS trajectory, which forms a trip for the car. Each trip contains a start coordinate, an end coordinate, and the distance driven by a car. Cars parking time can be inferred as the time between trips. To ensure the users' privacy, the trajectories are randomised by adding a noise distance between 50 and 500 meters to each trip's endpoints. The GPS trajectories of the cars were collected over three months, from September to November 2019 and is uniformly distributed across the country (Denmark) and vehicle segments. The GPS trajectories do not suffer from the biases identified in other EV studies, namely, having early adopters bias the behaviour in the data sets. In total, 32664 cars are observed in the capital region (Copenhagen), which accounts for 5.71% of the cars in the city (A total of 571627 cars for the period [Statistik-Banken, 2022]). In the observations period, the penetration rate of EVs in Copenhagen 1%, and for the fall of 2022, the penetration rate has increased to 2.5% [Statistik-Banken, 2022]. We visualise the number of daily trips for the entire period in Figure 8. In total, we have 1550509 trips with a median of 10 trips pr. car.

Charging Stations in Copenhagen To model the charging infrastructure in Copenhagen, we use the charging infrastructure from 2021. We scraped the infrastructure from uppladdning [2021], an open-source map containing locations of EV charging stations. The scraped chargers have different charging power ranging from slow chargers with 3.7 kW charging to fast chargers with 150 kW. These provide us with the locations and the power for each charging station in the city, which we use to determine where the ICE cars would have charged, assuming they were EVs.

Market shares of Electric vehicles Before we describe our battery and charging models, we generate the fleet of EVs based on the distribution of EVs in Denmark. To generate the EV fleet, we sample the EV characteristics for each car according to their market share distribution. We report the ten most popular EV models in Denmark can be seen in Table 5.

Generation of EV fleet Using the market shares, we generate a fleet of EVs from the ICE. Where each EV corresponds to an ICE, with the same trips. For each EV we keep track of the *SoC*, *Range* and *battery capacity* for the vehicle.

A.2 Battery Model

Firstly, we turn to our modelling of the Lithium ION batteries in the EV fleet. Initially, we set the SoC levels of the fleet to follow a truncated normal distribution as $SoC \sim \mathcal{N}(0.6, 0.2), 0.20 \leq SoC \leq 1$. We assume there is a linear relationship between the distance of a trip and State of charge consumption for a trip and model the SoC consumption (or the decrease in the SoC levels) as:

$$\text{Consumption pr. trip} = \frac{\text{Distance of trip}}{\text{Range of car type}}. \tag{22}$$

Ranking	Model	Count	Range (km)	Battery capacity (kWh)
1	Tesla Model 3 SR	8183	380.0	57.0
2	Renault Zoe	4050	315.0	52.0
3	Tesla Model S	3915	560.0	95.0
4	Volkswagen ID.3 EV	3353	350.0	58.0
5	Nissan Leaf	3033	225.0	37.0
6	Hunydai Kona BEV	2948	395.0	64.0
7	Volkswagen ID.4 EV	2473	400.0	77.0
8	Kira Niro EV	1890	370.0	64.0
9	BMW i3	1642	235.0	37.9
10	Volkswagen e-Up!	1370	205.0	32.3
-	Others	17399	313.0	60.0

Table 5: Top 10 most popular EV models in Denmark [Observatory, 2021] with manufacturing standards from [Database, 2021].

After one trip, we update the EV with the SoC for the next trip as:

$$\text{SoC}_{t+1} = \text{SoC}_t - \text{Consumption pr. trip}\,. \tag{23}$$

A.2.1 Charging decision

We model the charging decision with a smooth beta function. We evaluate the probability of charging after a trip as a CDF of a beta distribution with the initial x_i and the final SoC x_f levels. [Hipolito et al., 2022] The PDF of a beta distribution is

$$f_\beta(a, b; x) = \frac{x^{a-1}(1-x)^{b-1}}{\Gamma(a)\Gamma(b)/\Gamma(a+b)}\,. \tag{24}$$

We model the probability of charging with a $SoC \leq x$ as the CDF ($F_\beta(a, b; x)$) of the survival function

$$S_\beta(a, b; x) = 1 - F_\beta(a, b; x) = 1 - \int_0^x f_\beta(a, b; t)dt \tag{25}$$

Using this equation for the decision to charge can lead to counterintuitive examples of charging, where cars charge even at high levels of SoC. Therefore we make the vehicles context-aware by assessing the willingness to charge based on the initial SoC (x_i) and the final SoC (x_f) of a trip. We compute the willingness to charge based on the differences between the CDFs for the initial SoC and the final SoC, normalized to the probability of charging at the start÷

$$W_\beta\left(a, b; x_f, x_i\right) = \left[F_\beta\left(a, b; x_i\right) - F_\beta\left(a, b; x_f\right)\right] / F_\beta\left(a, b; x_i\right)\,. \tag{26}$$

Using the willingness to charge, we random draw if a car decides to charge. The parameters a and b are estimated via non-linear regression We use default parameters for the distributions, and the reader is referred to [Hipolito et al., 2022] for a larger discussion on the willingness to charge and the estimation of a and b.

A.3 Where to charge

The willingness to charge gives us a willingness score between 0 and 1. Based on the willingness score, we randomly draw if you charge or not. We employ a simple discrete choice model to decide where to charge, if the car needs to charge We identify the five closest chargers based on the trip end point and compute their utility as the distance between the endpoint of the trip and the charger location. For each station of the 5 closest, we draw the probability:

$$P_j = \frac{\exp(D_j)}{\sum \exp(D_j)}\,, \tag{27}$$

where D_j is the distance between the charging station and the end trip point the trip and P_j is the probability of going to station j. We then randomly select a charging station from the P_j of the five closest charging stations.

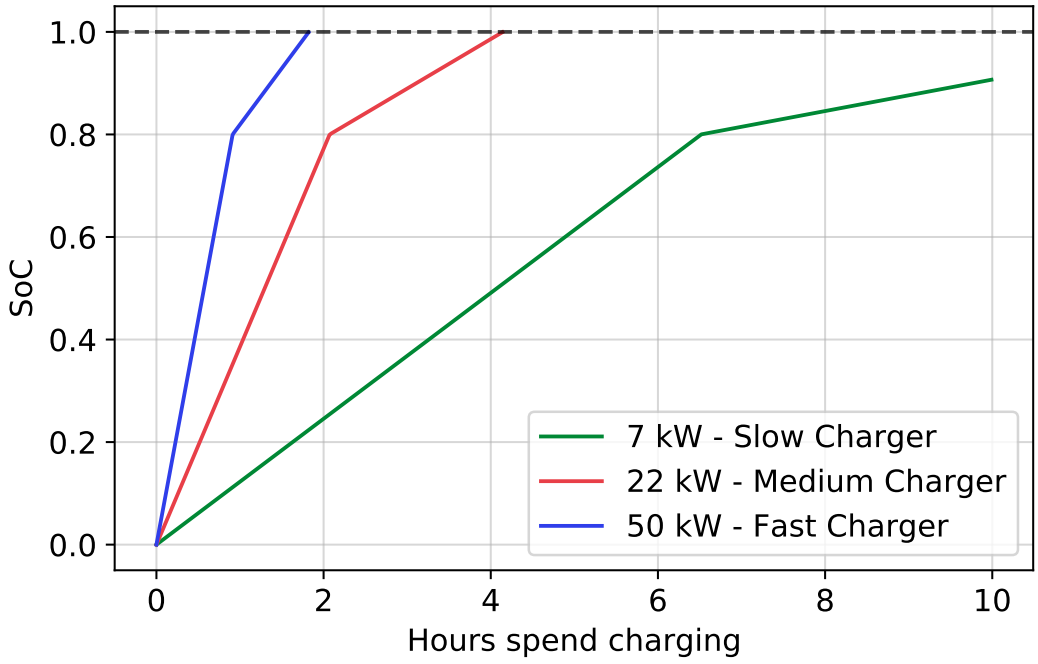

Figure 9: Charging curves for a *Tesla Model 3* with a battery capacity of 57 kWh and three different charging capacities. A 7kW slow charger, a 22 kW medium charger and a 50 kW fast charger.

A.3.1 Charging model

We model the decision to charge as a probabilistic choice between the Once a charger has been chosen, we approximate the charging of the EV with a piecewise linear model [Gjelaj et al., 2020]. The time spent charging will be dependent on the queue for the study. Firstly, we compute the time it takes for the car to have an SoC more than 80% as:

$$T_{80} = 0.8 \left(\frac{\text{Battery capacity} - SoC \cdot \text{Battery capacity}}{\text{Charger power}} \right) . \tag{28}$$

We then compute the new SoC for the car based on the following. In Figure 9 , we show an example of the charging equation for three different charger types:

$$\text{SoC}_{t+1} = \begin{cases} (\text{SoC}_t + \text{charging time} * \frac{\text{Charger power}}{\text{Battery capacity}}) & \text{if charging time} < T_{80} \\ 0.8 + 0.25((\text{charging time above } T_{80}) * \frac{\text{Charger power}}{\text{Battery capacity}}) & \text{else} \end{cases} . \tag{29}$$

Finally, we store the energy required for the charging. If a vehicle did not charge due to occupied charging stations, we assume it would have charged to 80% SoC and store this as censored demand.

A.4 Summary of the counterfactual study

Using the points made above, we conduct the counterfactual study. We vary the number of sample EVs to match the different penetration rates. In 2019, the penetration rate of EVs was roughly 1% and in 2022, is roughly 3%. The GPS trajectories themselves have a penetration rate of 5%. We run the study with three different queuing models. We sample the car distribution according to the count distribution in Table 5. Each car then follows the procedure outlined in Algorithm 1.

Algorithm 2 Overview of the counterfactual study.

Generate a fleet of electric vehicles.
Set queuing model.
Set SoC for the fleet of cars $SoC \sim \mathcal{N}(0.6, 0.2), 0.20 \leq SoC \leq 1$.
for each GPS trajectory **do**
    Find the car id of the GPS trajectory.
    Compute energy consumption for the car (Equation 22).
    Update SoC-level for the car (Equation 23).
    Compute willingness to charge for the car (Equation 26).
    Compute were to charge based on the end location of the trip (Equation 27).
    Add car to queue.
    Compute energy demand based on the time spent charging (Equation 29).
    Save the energy demand from the charging event.
end for

B Censoring across the different clusters

Queue	Cluster	Penetration Rate 1.0%	2.0%	3.0%	4.0%	5.0%
Gas-station	0	0.22%	1.26%	2.80%	5.08%	8.11%
	1	0.04%	0.09%	0.22%	0.49%	1.09%
	2	0.00%	0.00%	0.00%	0.18%	0.36%
	3	0.00%	0.05%	0.27%	0.22%	0.63%
	4	0.0v%	0.05%	0.14%	0.50%	1.40%
	5	0.00%	0.05%	0.18%	1.13%	2.17%
	6	0.00%	0.05%	0.09%	0.09%	0.36%
	7	0.00%	0.40%	0.67%	1.91%	3.09%
	8	0.00%	0.18%	0.31%	0.86%	2.22%
	9	0.04%	0.10%	0.45%	0.49%	1.22%
3-hour	0	2.08%	9.74%	20.80%	31.30%	41.96%
	1	0.27%	1.00%	4.08%	6.25%	11.69%
	2	0.00%	0.22%	0.18%	0.54%	1.45%
	3	0.36%	1.63%	2.72%	4.80%	9.15%
	4	0.09%	0.45%	1.72%	3.27%	5.66%
	5	0.14%	0.50%	1.22%	3.53%	5.89%
	6	0.04%	0.36%	0.58%	1.40%	2.62%
	7	0.27%	1.54%	3.72%	7.52%	10.24%
	8	0.63%	3.27%	7.11%	10.87%	13.18%
	9	0.27%	1.04%	2.22%	5.21%	8.47%
First come - First serve	0	4.17%	17.68%	38.70%	54.64%	61.03%
	1	0.77%	2.36%	7.11%	12.00%	20.29%
	2	0.04%	0.36%	0.58%	2.53%	3.12%
	3	0.86%	3.49%	6.57%	10.74%	16.31%
	4	0.13%	1.99%	4.17%	6.62%	11.28%
	5	0.22%	1.04%	5.71%	13.68%	24.33%
	6	0.22%	0.63%	1.31%	2.45%	6.57%
	7	0.54%	2.62%	7.43%	12.96%	20.16%
	8	1.27%	5.2%	12.96%	22.33%	31.17%
	9	0.59%	2.22%	4.80%	11.69%	16.67%

Table 6: Percentage of hours where the observed demand is censored across the different queues, penetration rates and clusters.